Demonstration of Enhanced Power Losses Characterization in Optical Networks

Alix May[1,2], Fabien Boitier[1], Aymeric Courilleau[1], Bichr Al Ayoubi[1], Patricia Layec[1]
[1]Nokia Bell Labs, Route de Villejust, 91620 Nozay, France. [2]LCTI Telecom Paris, Institut Polytechnique de Paris, 91120 Palaiseau, France
alix.may@nokia.com

Abstract: We generalize our receiver-based power losses characterization in a networking scenario. We show that combining monitored information from several lightpaths increases the estimation accuracy with an estimation error reduced from 1.40 dB to 0.50 dB.

1. Introduction

To bring optical network one step closer to marginless operation, massive monitoring needs to be deployed to gather as much information as possible about optical transmission and components impairments . It would allow the detection of soft failures as well as their localization, to make better and faster decisions in terms of operational maintenance and outage avoidance. Recent works on monitoring focused on soft failures detection and identification while localization during operation is often limited to span granularity [1]. Additional hardware is often required, notably for power losses characterization along an optical fiber with the use of optical time-domain reflectometers (OTDR). Recently, successful estimations of longitudinal power profiles were demonstrated from a single coherent receiver based on nonlinear back-propagation techniques [2]–[6]. Such techniques have been used to demonstrate the monitoring of additional phenomena [5] and processing has been implemented in FPGA [6]. This receiver-based monitoring provides distributed information along the whole lightpath.

In this study, we propose to investigate for the first time how to leverage the diversity of lightpaths in a networking scenario where each of them brings additional monitoring information to enhance the localization and the estimation of a power loss. In this paper, we first remind the receiver- and calibration-based power losses characterization. Then, we depict our experimental optical network setup. Next, we propose a generalization of the calibration step to ease deployment of the power losses characterization method over multiple lightpaths. Finally, we assess the enhancement in both location and estimation accuracy in our meshed network.

2. Reminder on power profile estimation and calibration method

The considered method relies on a power profile evaluation [2] and on a calibration to estimate the value of a power loss [3]. We proposed in [3] a model which gives the evolution of the peak amplitude $A_{\text{peak}}(z_0, T_0)$ of the anomaly indicator (AI) - the difference between a reference power profile and a monitored one - for a loss of value $(1 - T_0)$ located at the distance $z_0 - z^{(k)}$ from the position $z^{(k)}$ of the beginning of the k^{th} span:

$$A_{\text{peak}}(z_0, T_0) = C \cdot P_{\text{ref}}\left(z^{(k)}\right) \cdot (1 - T_0) \cdot 10^{-\alpha_{\text{fiber,dB}} \cdot \frac{z_0 - z^{(k)}}{10}} \quad (1),$$

with $\alpha_{\text{fiber,dB}}$ the fiber attenuation coefficient and P_{ref} the channel launch power of the k^{th} span in the reference profile. The loss distance $z_0 - z^{(k)}$ is given by the distance between AI peaks during calibration and monitoring phase. We introduced in [3] the calibration factor $C \cdot P_{\text{ref}}\left(z^{(k)}\right)$ which corresponds to the slope of the AI peak amplitude as a function of the loss value $(1 - T_0)$ for $z_0 = z^{(k)}$. It allowed us to determine this factor by emulating a known loss $(1 - T_0)$ at the beginning position $z_0 = z^{(k)}$, e.g. by varying the node output power. In [3], losses were inserted in a single span in a transmission with a single transmitter, a single receiver and a single launch power. Therefore, only one calibration factor was needed to estimate loss values. However, many parameters, such as the channel launch

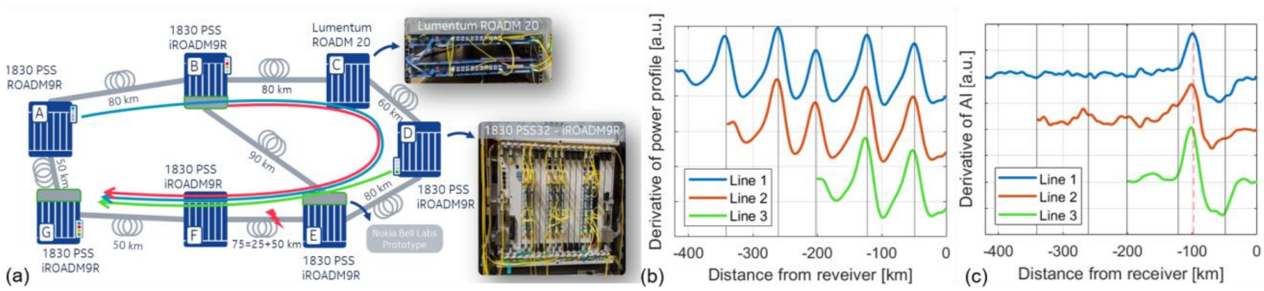

Fig. 1: a) Optical network testbed. From experiments: b) Derivative of power profiles for the three lines. c) Derivative of AI for the three lines when a loss of 4.5 dB occurs ~25 km after node E (vertical dashed red line). Vertical solid black line shows node position in (b) and (c).

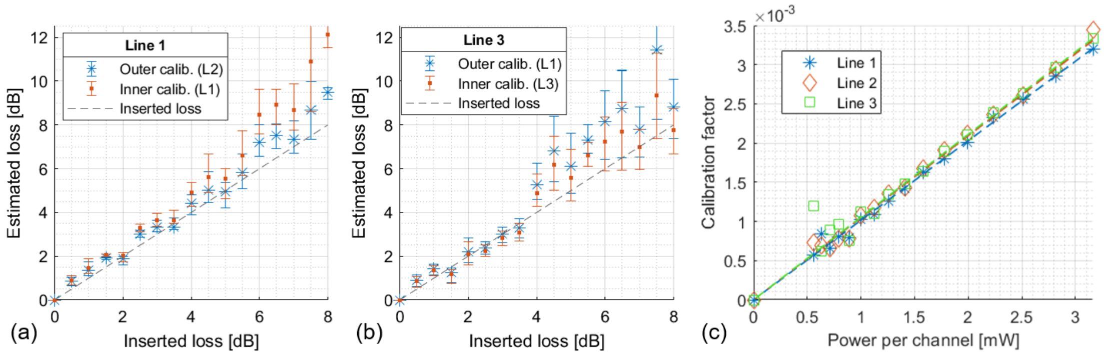

Fig. 2: a) Loss estimations from line 1 with calibration factors from line 2 and line 1. (b) Loss estimations from line 3 with calibration factors from line 1 and line 3. (c) Calibration factors versus launch power per channel. Dashed lines are linear fit of calibration factor for each line.

power or the total accumulated noise, could impact the height of the AI peak since it depends on the amount of generated nonlinear effects and on the quality of the received signal. In a network, where each lightpath will go through several spans and have different propagation distances, if no indication on the evolution of the calibration factor is given, the number of needed calibrations will be very high. Therefore, we first propose to extend and generalize the calibration method to multiple lightpaths and powers and then, to take advantage of the diversity of lightpaths - called “line” in the rest of the study - in a network to improve the quality of the results.

3. System description

To extend the calibration validity, we performed experiments on the meshed optical network testbed depicted in Fig. 1a. It is composed of seven nodes built from 3 vendors (Nokia, Lumentum and a prototype). The outer ring ranges 475 km of SSMF optical fiber. The testbed devices are operated via Netconf thanks to ADONIS Open agent [7], also enabling enhanced monitoring. We load the network with 20 ASE channels aligned on the 50GHz ITU grid. Three 32 GBaud PDM-QPSK channels are generated by a Nokia 1830 PSI-2T, named Line 1, 2 and 3 (in blue, red, and green), injected from distinct source nodes, A, B and D and received at the same destination node G after propagating through 421 km, 341 km and 202 km of optical fiber, respectively. These optical channels are both decoded by a Nokia 1830 PSI-2T and sent to an offline coherent receiver with 70 GHz bandwidth and 200 GSamples/s real-time oscilloscope. The network testbed is operated in a constant power mode, i.e., the output power of nodes is maintained constant regardless of the input power. Finally, a programmable variable optical attenuator (VOA) is placed after 24.02 km (OTDR estimation) of propagation in the penultimate fiber span, i.e., between node E and F, and enables the insertion of extra power loss (red lightning in Fig. 1a). When not specified, the channel launch power is 5 dBm.

4. Calibration generalization in an optical network

We compute for each loss and line 65000 raw power profiles. Each profile is computed using 2048 received samples. In Fig. 1b, we plot the derivative of the average reference power profiles for the 3 lines such that the position of the peaks corresponds to the position of the nodes (vertical solid black line). For each line, the calibration factor $C \cdot P_{\mathrm{ref}}\left(z^{(k=E)}\right)$ is obtained by varying the output power of the node E. Then we perform loss estimations by using the amplitude and position of the AI peaks. For example, in Fig. 1c, we plot the derivative of the AIs for each line for a 4.5 dB loss, all showing a peak around the position of the inserted loss (vertical dashed red line).

To reduce the number of required calibrations, we propose to use the same calibration factor for several lines. We perform loss estimation using 12000 raw profiles for line 1 and 3 with different calibration factors: one with the corresponding factor (inner calibration) and one with the factor of another line (outer calibration). We plot in Fig. 2a, (resp. Fig. 2b), the mean estimated loss (over 5 realizations) for line 1 versus inserted loss when the calibration factor of line 1 and 2 are used, (resp. for line 3 with factor of line 3 and 1). The errors bars correspond to the maximum and minimum estimated values. We notice that though the estimation is better when the inner calibration factor is used in Fig. 2b (red squares), in Fig. 2a, it is not the case. We attribute such discrepancy to the intrinsic error of the estimation which is of the same order of magnitude as the outer calibration error. Either way, we see that, confirming our proposition, the estimation remains accurate when using the calibration of a line with a different propagation distance, from 202 km (line 3) to 421 km (line 1), and different performance.

We also propose to extend the calibration factor validity to different launch powers. We determine $C \cdot P_{\mathrm{ref}}\left(z^{(k=E)}\right)$ for various span launch powers per channel, from 5 dBm (3.16 mW) to -2.5 dBm (0.56 mW). The results are reported for each line in Fig. 2c. We see that the calibration factor is proportional to the launch power, which validates the proposed formulation of the calibration factor as the product $C \cdot P_{\mathrm{ref}}\left(z^{(k=E)}\right)$ in [3] and allows us to rely only on the value of its first term C .

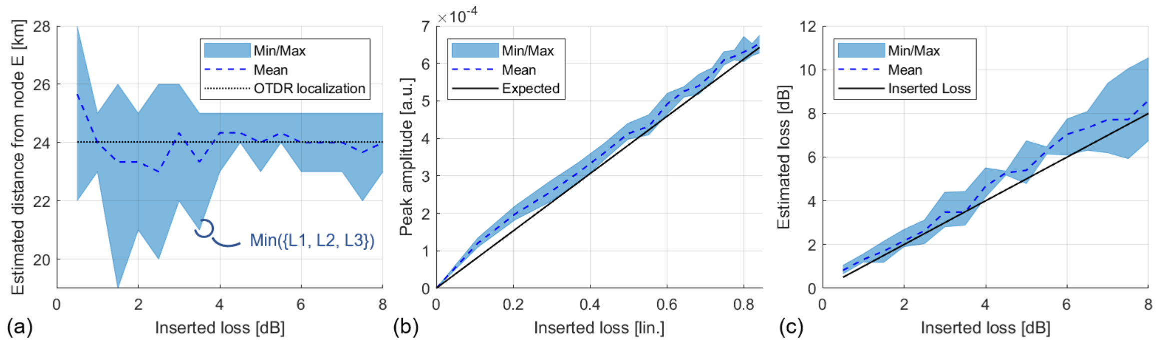

Fig. 3: Estimation statistics over Line 1, 2 and 3: a) Estimated distance of the losses from node as a function of inserted loss. b) Peak amplitude as a function of inserted loss. c) Estimated loss as a function of inserted loss

5. Loss characterization results

In an optical network, when an extra loss occurs in a span, several receivers would have estimated both its distance to node and its value. In monitored networks, we can combine these estimations to refine them and increase reliability by avoiding having to trust a single line. We perform another series of experiments, varying the VOA attenuation from 0.5 to 8 dB. In the following, the AIs are computed using 28000 raw profiles with a 1-km resolution and we use only one calibration factor (from Line 2). For each line and each loss, we estimate the distance from node E and loss value.

In Fig. 3a, we report the mean, maximum and minimum estimated loss distances from the node E over the three lines as a function of inserted losses. We circled a point which corresponds to an attenuation of 3.5 dB and is the minimum estimated distance of the three lines, equal to 21 km. We see that the mean estimated distance over lines is very close its measured value (by OTDR) 24.02 km. We observe that for small losses, the single line estimations (maximum or minimum) can be quite far away from the OTDR value. For instance, for a loss of 2.5 dB, the single line error in localization can be up to 4 km, while it is reduced to 1 km when the three estimations are averaged. Thus, estimation diversity helps reducing the localization error. This increase in localization accuracy will also reduce the error on the fiber propagation loss term in Eq.(1) and thus reduce the loss estimation error. In Fig. 3b, we report, in the same way, the peak amplitudes statistics over the three lines. We also plot the expected peak values obtained from Eq.(1) with the known position and values of the losses. We see that the difference between maximum and minimum values over the three lines is small, confirming the possibility to use a single calibration factor for the three lines for the estimation at $z_0 = 24.02$km. Finally, we plot in Fig. 3c, the maximum and minimum single line estimations as well as the estimations using the mean values of distance and peak amplitudes over the three lines (showed in Fig. 3a and 3b). We observe that taking these mean values to perform the estimation allows an improvement of the accuracy. For example, for an attenuation of 3 dB, the combined estimation error is 0.50 dB whereas one of the three lines alone gives an error of 1.40 dB. Overall, for all losses, the maximum error of the mean value is <1.0 dB, and <0.7 dB for losses <4 dB. This highlights the benefits of combining the results of several lines.

Conclusion

We propose in this paper a generalization of a power loss characterization method. We extend the use of the same calibration factor in two ways: i) for several lines with different transmitters, frequencies, and propagation distances, ii) for different powers. We also demonstrate that the combination of the monitored information from several lines enables to increase the accuracy of the localization and the loss value estimation. When using a single line for monitoring, the maximum error in localization could be up to 4 km. By combining 3 lines, we decrease this value to 1 km. In the same way, we reduce a maximum estimation error obtained with a single line of 1.40 dB to 0.50 dB with three lines.

References

[1] A. P. Vela *et al.*, 'Soft Failure Localization During Commissioning Testing and Lightpath Operation', *J. Opt. Commun. Netw.*, vol. 10, no. 1, p. A27, Jan. 2018.

[2] T. Tanimura *et al.*, 'Fiber-Longitudinal Anomaly Position Identification Over Multi-Span Transmission Link Out of Receiver-end Signals', *J. Lightwave Technol.*, vol. 38, no. 9, pp. 2726–2733, 2020.

[3] A. May *et al.*, 'Receiver-Based Experimental Estimation of Power Losses in Optical Networks', *IEEE Photon. Technol. Lett.*, vol. 33, no. 22, pp. 1238–1241, 2021.

[4] T. Sasai *et al.*, 'Simultaneous Detection of Anomaly Points and Fiber types in Multi-span Transmission Links Only by Receiver-side Digital Signal Processing', in *Optical Fiber Communication Conf.*, San Diego, California, 2020, p. Th1F.1.

[5] S. Gleb *et al.*, 'Fiber Link Anomaly Detection and Estimation Based on Signal Nonlinearity', *European Conference on Optical Communication*, p. Tu2C2.5, 2021.

[6] T. Tanimura *et al.*, 'Concept and implementation study of advanced DSP-based fiber-longitudinal optical power profile monitoring toward optical network tomography [Invited]', *J. Opt. Commun. Netw.*, vol. 13, no. 10, p. E132, 2021.

[7] Ll. Gifre *et al.*, 'Demonstration of Monitoring and Data Analytics-triggered reconfiguration in partially disaggregated optical networks', in *Optical Fiber Communication Conf.*, San Diego, California, 2020, p. M3Z.19.